

***Ab initio* search for a high permeability material based on bcc iron**S. Ostanin,¹ J. B. Staunton,¹ S. S. A. Razee,² C. Demangeat,³ B. Ginatempo,⁴ and Ezio Bruno⁴¹*Department of Physics, University of Warwick, Coventry CV4 7AL, United Kingdom*²*Department of Physics, University of Kuwait, SAFAT 13060, Kuwait*³*Institut de Physique et Chimie des Matériaux de Strasbourg, 23, rue du Loess, 67034 Strasbourg Cedex 2, France*⁴*Dipartimento di Fisica and Unità INFN, Università di Messina, Salita Sperone 31, I-98166 Messina, Italy*

(Received 9 September 2003; published 23 February 2004)

Using the fully relativistic spin-polarized Korringa-Kohn-Rostoker method, we study the prototypical soft magnet, bcc iron. We investigate how its magnetic anisotropy (MAE) varies as a function of volume, band filling, and tetragonal distortions of the crystal lattice. We follow the trends of the linear magnetostriction and magnetic permeability. We find that a slight reduction in band filling and modest lattice expansion produces a significant magnetic softening of this model system. We explore whether this situation can be realized by doping bcc Fe with vanadium. Treating the compositional disorder with the coherent potential approximation, we calculate the magnetic anisotropy and magnetostriction trends of iron-rich $\text{Fe}_{1-c}\text{V}_c$ disordered alloys and find the behavior to accord with the predictions from the bcc Fe model. In particular we find that for $c \approx 0.1$ the MAE is very small and the linear magnetostriction is zero. We propose $\text{Fe}_{0.9}\text{V}_{0.1}$ as a high permeability material. Fair agreement with experimental values for the MAE and magnetostriction of both Fe and FeV is found.

DOI: 10.1103/PhysRevB.69.064425

PACS number(s): 75.30.Gw, 71.20.Be, 75.50.Bb

I. INTRODUCTION

Soft ferromagnetic materials allow changes in magnetization to occur easily in weak fields, i.e., they have high magnetic permeability. They find applications ranging from electrical power generation and magnetic shielding to magnetic recording heads and spin valve devices.^{1,2} For a magnet to be “soft,” changes to the overall magnetization must be able to happen easily. This implies that its magnetic anisotropy constants K are very small so that the energies of domain walls are low. The internal stresses caused by such changes must also be minimal so that the magnetostriction coefficients λ are as small as possible. Roughly, the magnetic permeability $\mu \propto M_s^2/K_{eff}$, where M_s is the saturation magnetization and K_{eff} is a measure of magnetic anisotropy and magnetostriction, $K_{eff} = K_{eff}(K, \lambda)$.

In a binary component soft magnetic material, K and λ do not generally pass through or near zero together. For example, in iron-nickel permalloys, K and λ pass through zero at different compositions and the addition of a third or fourth component is required to achieve “the focus of zero.”³ This is done practically by checking hundreds of samples.³ In this paper, we explore the variation of these two factors K and λ using *ab initio* spin polarized, relativistic electronic structure calculations and attempt to design optimally soft magnetic materials. For the first such study we choose an uncomplicated system, namely the prototypical soft magnetic material, bcc iron, and examine how its K and λ would vary if its lattice spacing (volume) and number of valence electrons (band filling) could be altered. We find that on reducing the band filling marginally and increasing the volume slightly, iron’s magnetic properties soften considerably. We then test this model by an explicit study of iron-rich Fe-V alloys and find the optimal composition for smallest K and λ . In a subsequent paper⁴ we carry out an analogous investigation where we start from $\text{Ni}_{0.75}\text{Fe}_{0.25}$ permalloy and consider the

addition of Cu and Mo dopants.

Fe-V alloys are also magnetic materials of significant interest in their own right. The rather small lattice mismatch between Fe and V has made Fe/V thin film and multilayered systems very attractive^{5–14} for studies of the interconnections between structure, magnetism, and chemical order. The observations of magnetocrystalline anisotropy (MAE) in Fe/V films show¹⁵ the easy axis to be along [100] and the magnitude of the MAE to be small, comparable to that of bulk bcc Fe. Electronic structure density-functional calculations (DFT) also calculate the easy axis to be [100] in Fe/V.¹⁶ Despite this recent work on Fe/V thin films much less is known about the magnetic anisotropy of the bulk alloys. Here we study the magnetic anisotropy of $\text{Fe}_{1-c}\text{V}_c$ as a function of both small concentrations c of V and also lattice distortions. It is known experimentally that the saturation magnetostriction λ_s of bcc Fe is negative. Its magnitude decreases when lightly doped with V and with around 5 at. % V, λ_s , measured in polycrystalline samples,¹⁷ is almost zero. For further addition of V, λ_s changes its sign to positive reaching the value of 8×10^{-6} at 15 at. % V. There is thus a particular Fe-rich concentration of $\text{Fe}_{1-x}\text{V}_x$ where the magnetostriction is as small as possible while the magnetocrystalline anisotropy constant K remains very low for this magnetically soft alloy. Both these attributes ($K \approx 0$ and $\lambda \approx 0$) promote high permeability and along with their high Curie temperatures and saturation magnetizations enhance the uses of iron-rich Fe-V alloys.

In the following section we briefly summarize our approach for calculating the magnetic anisotropy of metals and alloys. It is based on the spin-polarized relativistic Korringa-Kohn-Rostoker (SPR-KKR) DFT method, within the coherent-potential approximation (CPA) (Refs. 18,19) for alloys. We show how magnetostriction can also be found. In the following section we use the method to study the variation of the MAE of bcc iron with band filling, volume, and

tetragonal (t) distortion. We find the MAE “landscape” to be highly structured and to possess a region where high permeability is possible. We show in the penultimate section on MAE calculations for $\text{Fe}_{1-c}\text{V}_c$ alloys that, for small c , these high permeability properties appear. The final section summarizes and concludes.

II. MAGNETIC ANISOTROPY OF METALS AND ALLOYS

Magnetic anisotropy is caused largely by spin-orbit coupling. Both the origin of this effect, as well as the magneto-static effects which determine domain structure, can be shown from the relativistic generalization of spin-density-functional (SDF) theory.²⁰ From the formal starting point of the quantum electrodynamics of an electron interacting with an electromagnetic field, the ground-state energy of a system is the minimum of a functional of the charge and current densities—a minimization which is achieved, in principle, by the self-consistent solution of a set of Kohn-Sham Dirac equations for electrons moving in fields dependent on the charge and current densities. Following approximations for exchange correlation and the Gordon decomposition of the current into orbital and spin pieces, the spin-orbit coupling effects upon the electronic structure can be represented. (The magnetostatic shape anisotropy is also described from within the same theoretical framework²⁰ but not considered for cubic materials of this paper.)

Most theoretical investigations of magnetocrystalline anisotropy and calculations of the anisotropy constants K place their emphasis on spin-orbit coupling effects using either perturbation theory or a fully relativistic theory, e.g., (Refs. 21,18). Typically the total energy, or the single-electron contribution to it (if the force theorem is used²²), is calculated for two magnetization directions, \hat{e}_1 and \hat{e}_2 separately, i.e., $F_{\hat{e}_1}$, $F_{\hat{e}_2}$, and then the MAE, ΔF , is obtained by subtracting one from the other, i.e.,

$$\int_{\varepsilon_F^1} \varepsilon n_{\mathbf{e}_1}(\varepsilon) d\varepsilon - \int_{\varepsilon_F^2} \varepsilon n_{\mathbf{e}_2}(\varepsilon) d\varepsilon, \quad (1)$$

where ε_F^1 , ε_F^2 are the Fermi energies when the system is magnetized along the directions \mathbf{e}_1 and \mathbf{e}_2 , respectively, and $n_{\mathbf{e}_{1(2)}}$ the electronic density of states. However, the MAE is a small part of the total energy of the system, in many cases of the order of μeV and it is numerically more precise to calculate the difference directly.¹⁸ We follow this rationale here for the study of soft magnetism and calculate the MAE from

$$\Delta F = - \int_{\varepsilon_F^1} [N(\varepsilon; \mathbf{e}_1) - N(\varepsilon; \mathbf{e}_2)] d\varepsilon - \frac{1}{2} n(E_{F_2}; \mathbf{e}_2) (E_{F_1} - E_{F_2})^2 + \mathcal{O}(E_{F_1} - E_{F_2})^3, \quad (2)$$

where $N(\varepsilon; \mathbf{e})$ represents the density of states of a system magnetized along \mathbf{e} integrated up to energy ε .

In most of the cases, the second term is expected to be very small compared to ΔF . The first term which contains the predominant contribution to ΔF needs to be evaluated accurately. For a binary component disordered alloy $A_{1-c}B_c$

the MAE can be written using the Lloyd formula for the integrated density of states in Eq. (2) to get

$$\begin{aligned} \Delta F = & -\frac{1}{\pi} \text{Im} \int_{\varepsilon_F^1} d\varepsilon \left[\frac{1}{\Omega_{BZ}} \right. \\ & \times \int d\mathbf{k} \ln \| I + [t_c^{-1}(\mathbf{e}_2) - t_c^{-1}(\mathbf{e}_1)] \tau_c(\mathbf{k}; \mathbf{e}_1) \| \\ & + (1-c) \{ \ln \| D_A(\mathbf{e}_1) \| \\ & - \ln \| D_A(\mathbf{e}_2) \| \} + c \{ \ln \| D_B(\mathbf{e}_1) \| - \ln \| D_B(\mathbf{e}_2) \| \} \left. \right] \\ & - \frac{1}{2} n(E_{F_2}; \mathbf{e}_2) (E_{F_1} - E_{F_2})^2 + \mathcal{O}(E_{F_1} - E_{F_2})^3 \quad (3) \end{aligned}$$

In Eq. (3), $t_c(\mathbf{e}_1)$ and $t_c(\mathbf{e}_2)$ are the SPR-KKR-CPA t matrices for magnetization along \mathbf{e}_1 and \mathbf{e}_2 directions, respectively, and $\tau_c(\mathbf{k}; \mathbf{e}_1)$ is the scattering path operator

$$\tau_c(\mathbf{k}; \mathbf{e}_1) = [t_c^{-1}(\mathbf{e}_1) - g(\mathbf{k})]^{-1}, \quad (4)$$

and τ_c^{00} is its integral over the Brillouin zone. $D_A(\mathbf{e}_1)$ is found from

$$D_A(\mathbf{e}_1) = [I - \tau_c^{00}(\mathbf{e}_1) \{ t_c^{-1}(\mathbf{e}_1) - t_A^{-1}(\mathbf{e}_1) \}]^{-1}, \quad (5)$$

with similar expressions for $D_A(\mathbf{e}_2)$, $D_B(\mathbf{e}_1)$, and $D_B(\mathbf{e}_2)$. Note that $t_A(\mathbf{e}_2)$ and $t_B(\mathbf{e}_2)$, the single site t matrices for A and B atoms, respectively, spin-polarized along \mathbf{e}_2 , can be obtained directly from $t_A(\mathbf{e}_1)$ and $t_B(\mathbf{e}_1)$, respectively, by simple rotational transformations.¹⁸ Further details, calculational techniques, and results of numerical tests can be found elsewhere.^{18,19} These include a description of the method of Brillouin-zone integration we use. It is an adaptive quadrature procedure so that the integrals can be computed to a prescribed accuracy. We have shown^{18,19} that the numerical accuracy of our SP-KKR-CPA calculations is to within $0.1 \mu\text{eV}$ (or 10^4 erg/cm^3) and thus the scheme is suited for studies of magnetically soft alloys.

Magnetostriction

The magnetostriction constant λ_{001} represents the relative change of length ($\delta l/l$) measured along $[001]$ when an external magnetic field is applied parallel to the direction of observation. For a cubic system λ_{001} appears in the equation²³

$$B_1 = -\frac{3}{2} \lambda_{001} (C_{11} - C_{12}), \quad (6)$$

where B_1 is the rate of change of the MAE, $F_{001} - F_{100}$, with tetragonal strain $t_{[001]}$ along $[001]$, at $t_{[001]} = 0$. C_{11} and C_{12} are the cubic elastic constants which can be expressed in terms of the tetragonal shear (C') modulus: $C' = (C_{11} - C_{12})/2$. λ_{001} of Fe, calculated from this expression using a full-potential DFT method, is rather large in comparison with experiment.^{24,25} Freeman and co-workers have estimated $C_{11} - C_{12}$ by fitting their calculated total energies to simple quadratic functions of the tetragonal distortion $t_{[001]}$ and extracting B_1 from the gradient of the energy difference

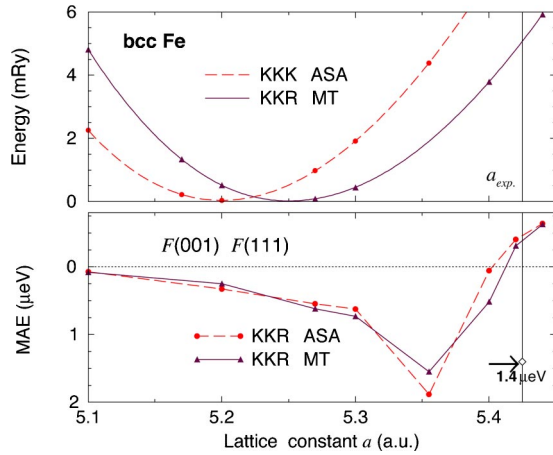


FIG. 1. Total energy of Fe with the lattice constant variation is shown in the upper panel (a). The energies, calculated using the SPR-KKR technique with MT and ASA potentials, are shifted to the common zero energy at the equilibrium a . The experimental a is marked as well. In the lower panel (b), the MAE between the [001] and [111] directions of magnetization, within the MT and ASA, are plotted against a . The experimental MAE value of $1.4 \mu\text{eV}$ is marked by an arrow.

$F_{e=(001)} - F_{e=(100)}$ with respect to $t_{[001]}$. In the case of Fe this approach produces an estimate of λ_{001} greater than that found experimentally.^{26,27} Rather than to estimate $C_{11} - C_{12}$ from such total-energy calculations, here we use experimental values if necessary, use the atomic sphere approximation (ASA) for the self-consistent one-electron potentials and track the trends of the magnetostriction from our relativistic electronic structure calculations of B_1 .

III. THE MAGNETIC ANISOTROPY AND MAGNETOSTRICTION OF bcc Fe

We investigate the dependence of the MAE of Fe on volume and also on volume conserving tetragonal distortions to obtain B_1 . We also see how the MAE changes when the Fermi energy is shifted to mimic roughly the effect of alloying.

First we recall how the equilibrium volume of Fe can be determined. In Fig. 1(a), the calculated total energy of Fe is shown as a function of the lattice parameter a . Typically for DFT calculations with the local density approximation (LDA), the equilibrium volume with $a = a_0$ is underestimated somewhat. This underestimation is less for muffin-tin (MT) potential calculations than when the ASA is used. From the shape of the total-energy curve, the calculated bulk modulus of 2.34 Mbar is in reasonable agreement with experiment and also with all DFT results previously reported. In Fig. 1(b), the magnitude of MAE ($F_{001} - F_{111}$) is plotted against the lattice spacing a of the bcc lattice. The easy axis is directed along [001] when $a < 5.4$ a.u. and along [111] if $a > a_{exp}$. At around the theoretical equilibrium volume of Fe, the easy axis direction along [001] is consistent with experiment while the predicted MAE of $\sim 0.6 \mu\text{eV}$ is almost half the observed one. Note the sharp change in the MAE for $5.35 < a < 5.42$. This might go some way to explain the ap-

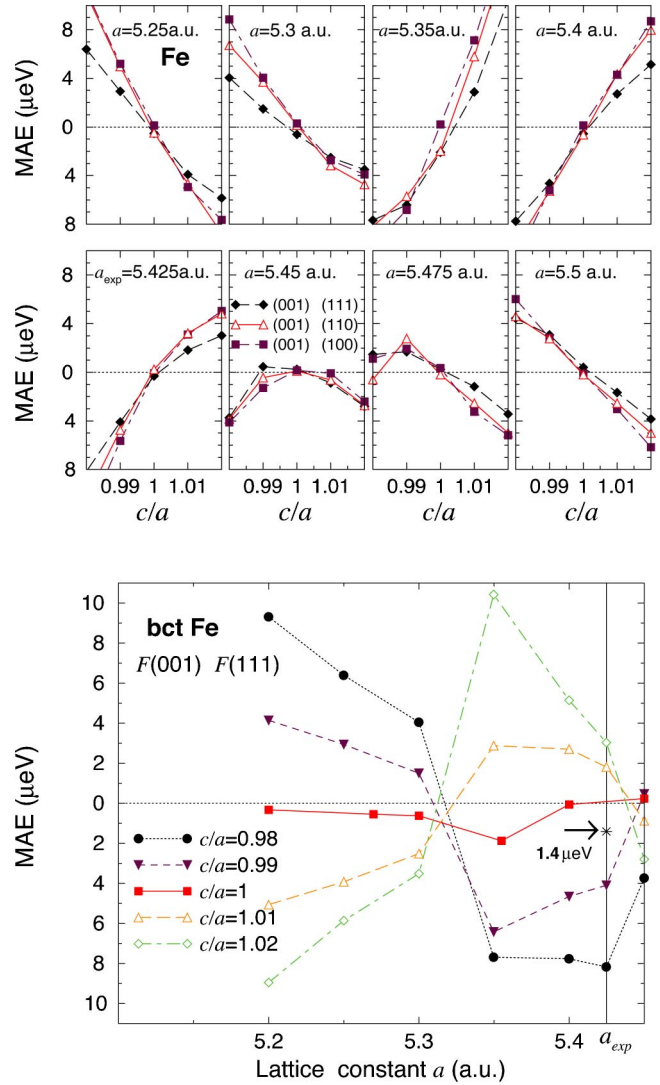


FIG. 2. (a) The variation of MAE in pure Fe with volume-conserving tetragonal deformations for a series of different volumes. The slope at $c/a = 1$ gives the coefficient B_1 . (b) The variation of MAE with volume for a series of volume conserving tetragonal distortions.

parent discrepancies among the many published MAE calculations for bcc Fe, e.g., Refs. 18, 28, and 29. If all the MAE calculations are numerically accurate, e.g., the various Brillouin-zone integrations are numerically converged, then the MAE values may still be at odds if the lattice spacing parameters differ.

The t distortions, which break the cubic symmetry making the [001] and [100] directions nonequivalent, may increase the MAE significantly. In Fig. 2(a), we plot the MAE of Fe as the c/a ratio is altered. The slopes of these graphs around $t = 0$ or $c/a = 1$ produce the coefficient B_1 related to the magnetostriction. The eight a values were chosen to illustrate the sensitivity of MAE to volume changes and t deformations. For each a , labeled in the corresponding panel of Fig. 2(a), we plot all three symmetry-allowed MAE curves: $\Delta F = F_{001} - F_{111}$, $F_{001} - F_{110}$, and $F_{001} - F_{100}$. At the equilibrium lattice constant ($a_0 = 5.25$ a.u.) the slopes of all three

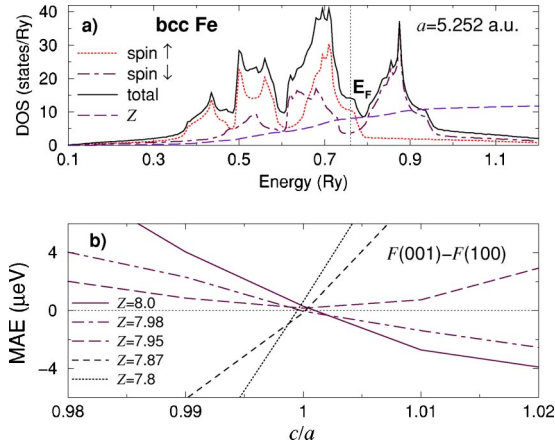


FIG. 3. Spin projected and total DOS of pure Fe, calculated for the equilibrium lattice parameter, are shown in the upper panel (a) together with the band-filling curve Z . In the (b) panel, the variation of MAE in Fe with volume-conserving tetragonal deformations is shown for a series of different band fillings.

curves are negative and then, between 5.3 a.u. and 5.35 a.u., they change becoming positive at the experimental lattice constant and, finally, at $a > 5.475$ a.u. $B_1 = \delta\Delta F / \delta(c/a)$ becomes negative once more. Figure 2(b) displays the variations of the MAE for six t distortions as a function of lattice spacing. From experimental measurements³⁰ on Fe, $C_{11} = 2.41 \times 10^{11}$ N/m² and $C_{12} = 1.46 \times 10^{11}$ N/m². The experimental value of λ_{001} is 26×10^{-6} . Substituting these data into Eq. (6) yields an experimental value of B_1 of approximately -3.7×10^6 J/m³ or -260 μ eV/atom to compare with the calculated B_1 at the theoretical equilibrium lattice spacing extracted from Fig. 2(a) of -500 μ eV/atom.

It is instructive to examine how the MAE and B_1 vary if the band filling or E_F position is altered. The results for Fe are shown in Fig. 3. In panel (a) of Fig. 3, the Fe electronic density of states (DOS) at a_0 is plotted together with the band-filling curve Z , which equals the number of valence electrons at given energy. In panel (b) of Fig. 3, the MAE, $F_{001} - F_{100}$, is shown as a function of c/a for different degrees of band filling. With fully filled bands ($Z=8$ electrons), the sign of $\delta\Delta F / \delta(c/a)$ is negative. If $Z=7.95$ electrons (corresponding to $E_F - 0.05$ eV) soft magnetic-material properties are developed so that the MAE, $\Delta F = F_{001} - F_{111}$, is tiny ($=0.62$ μ eV for $c/a=1$) and the slope $B_1 \sim 0$ implying a very small magnetostriction ($\lambda \approx 0$). Further lowering of E_F causes B_1 to become positive, increasing the magnitude of λ .

Our model deals with perfect crystal structures, point lattice defects, such as native vacancies, may affect the electronic properties of the material in a similar way to the band-filling effect. Thus, vacancy-containing defect structures of real materials may be another reason why DFT tends to underestimate the MAE value of Fe. By modeling the magnetovolume and band-filling effects as above, we have demonstrated that the Fe host matrix can breed soft magnetic properties. Our results suggest that Fe-rich binary alloys, $\text{Fe}_{1-c}\text{A}_c$, may lead to high permeability conditions when $Z_A < Z_{\text{Fe}}$ and $a_A > a_{\text{Fe}}$. Doping Fe with V complies with

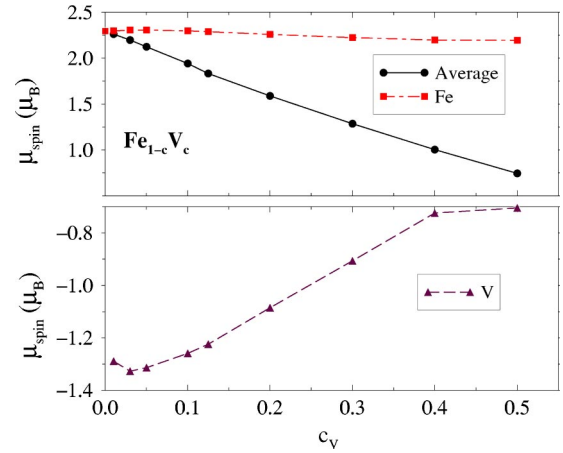


FIG. 4. Average and site-projected spin magnetic moments of Fe and V in the randomly disordered bcc $\text{Fe}_{1-c}\text{V}_c$ alloys as calculated by SPR-KKR-CPA.

these conditions and so in the following section we look at iron-rich Fe-V alloys.

IV. THE MAGNETIC ANISOTROPY AND MAGNETOSTRICTION OF $\text{Fe}_{1-c}\text{V}_c$ —A HIGH PERMEABILITY IRON-RICH ALLOY

As the first step, one-electron potentials for bcc- $\text{Fe}_{1-c}\text{V}_c$ randomly disordered bulk alloys were calculated self-consistently, using the SPR-KKR-CPA technique^{18,19} for the concentration range $1 < c < 50$ at. % V. The unit-cell volume was fixed at the experimental volume of each concentration. Exchange and correlation were accounted for on the basis of DFT in the local density approximation (LDA). The average and site-projected spin magnetic moments of $\text{Fe}_{1-c}\text{V}_c$ are given in Fig. 4. The average spin moment of this alloy decreases monotonically with increasing V concentration to the value of $0.74\mu_B$ at $c=0.5$. However the site-projected magnetic moments do not vary monotonically. The Fe spin magnetic moment varies between $2.31\mu_B$ and $2.19\mu_B$ as c increases between $0 < c < 0.5$, with a maximum value of $2.31\mu_B$ at $c=0.05$. In the Fe-rich alloys, the V spin moment is also nonmonotonic: it starts at $-1.29\mu_B$, reaching the value of $-1.33\mu_B$ at $c=0.03$ and, with further increases of c , the V moment drops to $-0.71\mu_B$ at $c=0.5$. Our results are in good agreement with both neutron-diffraction experiments on $\text{Fe}_{1-c}\text{V}_c$ (Ref. 31) and also previous *ab initio* calculations.^{32,33}

The properties of nonmagnetic d metals, dissolved substitutionally in ferromagnetic hosts, have been well documented.^{34,35} When early d metals, such as V, substitute host Fe atoms in the bcc structure, an antiparallel alignment of the spin orientation on the impurity site is expected. This situation also holds for the concentrated Fe-V alloy system.^{33,36} In Fig. 5, we plot the DOS of $\text{Fe}_{0.5}\text{V}_{0.5}$ and $\text{Fe}_{0.95}\text{V}_{0.05}$. The DOS curves, projected onto the Fe site, show a bandwidth similar to that of V but, in contrast to its Fe partner, the V d -band DOS is rather featureless. Any differences in the DOS between $\text{Fe}_{0.5}\text{V}_{0.5}$ and $\text{Fe}_{0.95}\text{V}_{0.05}$, which can be seen in Fig. 5, occur simply because the con-

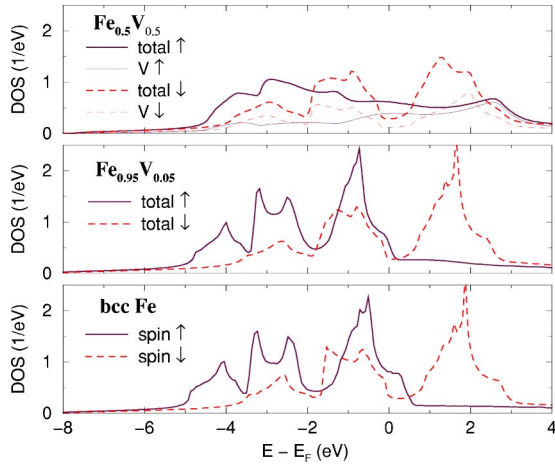


FIG. 5. Spin-projected DOS of pure Fe shown in the lower panel in comparison with the DOS of the $\text{Fe}_{0.5}\text{V}_{0.5}$ and $\text{Fe}_{0.95}\text{V}_{0.05}$ binary alloys plotted in the upper and middle panels, respectively.

centration c is changed. At small c , the spin-projected DOS of $\text{Fe}_{1-c}\text{V}_c$ approaches the corresponding DOS shape of pure Fe.

To confirm the expectation from the bcc Fe study that the magnetostriction of $\text{Fe}_{1-c}\text{V}_c$ should decrease with increasing V concentration, in Fig. 6 we plot $F_{001} - F_{100}$, calculated using “frozen” ASA potentials, as the c/a ratio is altered. For V concentrations of $0 < c < 0.1$, when $c/a < 1$, the easy axis is along [001] and when $c/a > 1$, it lies along [100]. For this concentration range, the magnitude of MAE increases almost linearly with t deformation and has its greatest values of several μeV at $c = 0.03$. For this concentration the magnetic spin moments and polarizations are maximum as shown in Fig. 4. At around 10 at. % V, the MAE magnitude, plotted in Fig. 6, decreases significantly and the easy axis changes its direction in such a way that for $c > 0.12$ the [100] becomes the easy axis when $c/a < 1$ whereas the axis along [001] is favored for the case of elongation ($c/a > 1$).

We confirm that the easy axis is [100] with Fig. 7. It shows the energy differences, ΔF 's, between the [111] (or [110]) magnetization directions and the easy axis, which is

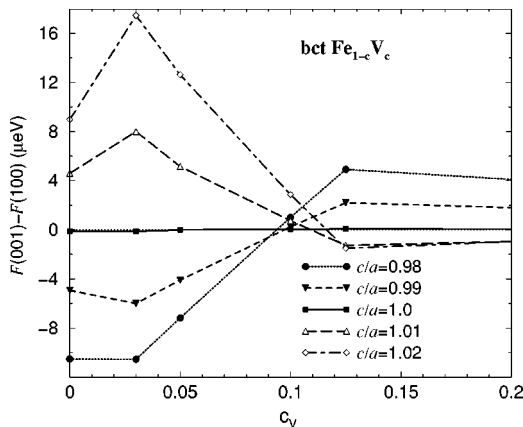


FIG. 6. The MAE, $\Delta F = F_{001} - F_{100}$, of disordered $\text{Fe}_{1-c}\text{V}_c$, shown as a function of V concentration for six different tetragonal c/a variations.

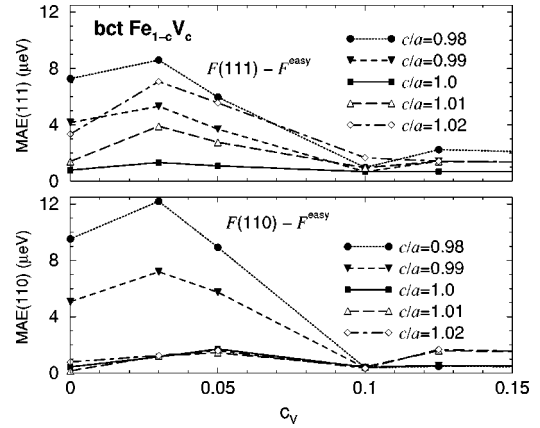


FIG. 7. The MAE's, ΔF 's, between the [111] ([110]) magnetization direction and that along the easy axis of $\text{Fe}_{1-c}\text{V}_c$, shown in the upper (lower) panel as a function of c for six different tetragonal c/a variations.

always directed either along the [001] or [100] cubic-lattice edges, depending on the c/a deformations and V concentration (see, Fig. 6). As Fig. 7 shows, the magnetic properties of the $\text{Fe}_{0.9}\text{V}_{0.1}$ alloy stand out from those of the other compositions. It is a very soft magnet; (i) the easy-axis direction switches and (ii) the rate of change of ΔF with the t deviation, (c/a), B_1 , changes sign from positive to negative. In Fe-rich Fe-V disordered alloys ($c < 0.1$), $B_1 > 0$, as shown in the three lower panels of Fig. 8. At around $c = 0.1$, B_1 is close to zero so that with increasing V content, for $c > 0.1$, B_1 becomes negative. Since $C_{11} - C_{12} > 0$ in this material, the sign of λ_{001} is totally defined by variation of MAE with the t deformations B_1 . Hence, for the $c = 0.1$ composition, the magnetostriction coefficient of this Fe-V alloy, $\lambda_{001} \rightarrow 0$ while the MAE value remains low enough for this alloy to develop high permeability.

There is experimental evidence for this behavior. For $\text{Fe}_{1-c}\text{V}_c$ alloys, although the magnetostriction coefficient λ_{001} is not available, measurements of the saturation magnetostriction λ_s have been reported.¹⁷ λ_s changes sign at

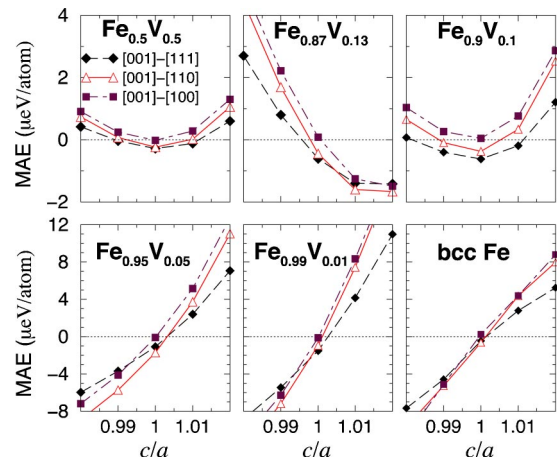


FIG. 8. The MAE's, ΔF 's, of disordered $\text{Fe}_{1-c}\text{V}_c$ alloys as a function of tetragonal deformations for six concentrations. The experimental lattice parameters are used.

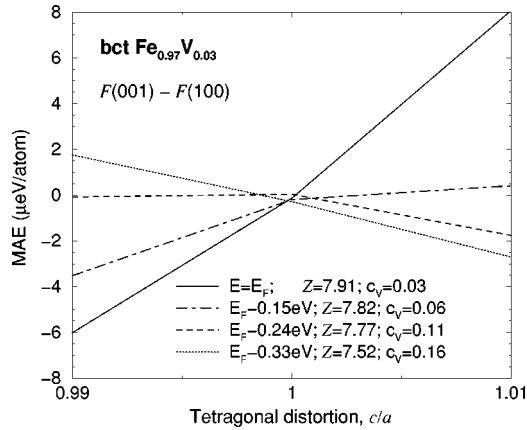


FIG. 9. The MAE of $\text{Fe}_{0.97}\text{V}_{0.03}$ as a function of the t deformations for four different band fillings.

around the 5 at. % V composition. Since λ_{001} is its most significant component, λ_s (Ref. 37) should also change its sign as the concentration of V is varied in this region.

Our SPR-KKR-CPA calculations include the direct modeling of the band-filling and magnetostriction effects. The magnetovolume effect is also presented here since we use the experimentally observed lattice parameters which increase slightly with V doping. To separate out and examine the band-filling effect we now show the dependence of the MAE of $\text{Fe}_{0.97}\text{V}_{0.03}$ on the number of electrons Z by varying the E_F in this alloy. The results are shown in Fig. 9 for the variation of the MAE with c/a for four different Z 's. From the MAE calculations of pure Fe, we know that the lattice constant is an important factor. At the experimental a and with the correct E_F for this alloy $Z = (1-c) \times 8 + c \times 5 = 7.91$ when $c = 0.03$. With decreasing Z , first $B_1 \rightarrow 0$ at $c \sim 0.1$ and then, as Z decreases further, B_1 changes sign. Soft magnetic proper-

ties are developed at $c \sim 0.1$. Thus, the simple band-filling model reproduces rather accurately the result of our direct calculations.

V. SUMMARY

Calculations of the magnetic anisotropy and the trends for magnetostriction in bcc Fe and Fe-V alloys have been carried out, using the fully relativistic spin-polarized KKR method and CPA alloy theory. The suitability of this method to model magnetic anisotropy in soft magnetic materials has been demonstrated. The MAE calculations for pure Fe are in a fair agreement with experiment. The linear magnetostriction coefficient λ_{001} , estimated from theory, shows also an acceptable agreement with the observations. The trends for magnetic softening by varying the volume and band filling and also straining the lattice tetragonally have been presented.

Our results for bcc Fe and recent experiments have directed us to look at iron-rich Fe-V as potential soft magnets. We have managed to follow the trends in our Fe calculations to find a potential iron-rich $\text{Fe}_{1-c}\text{V}_c$ alloy with zero magnetostriction. We have shown that the linear magnetostriction changes sign as c approaches 0.1. Since the MAE is very small for this composition we predict a very high permeability for this alloy. Combinations of Fe and V have extensive credentials as useful film and multilayered systems and $\text{Fe}_{0.9}\text{V}_{0.1}$ may prove to be a good high permeability film material, possibly competitive with those which are permalloy based. Such films might be realized from epitaxial growth on templates such as Fe(100), V(100), and Cr(100).

ACKNOWLEDGMENTS

We acknowledge support from the EPSRC (UK) and computing resources from the Center for Scientific Computing at the University of Warwick.

- ¹L. Krusin-Elbaum, T. Shinauchi, B. Argyle, L. Gignac, and D. Weller, *Nature (London)* **410**, 444 (2001).
- ²S.P. Li, W.S. Lew, A.A.C. Bland, L. Lopez-Diaz, M. Natali, C.A.F. Vaz, and Y. Chen, *Nature (London)* **415**, 600 (2002).
- ³T. Wakiyama, in *Physics and Engineering Applications of Magnetism*, edited by Y. Ishikawa and N. Miura, Springer Series in Solid State Sciences Vol. 92 (Springer-Verlag, Berlin, 1991), p. 133.
- ⁴S. Ostanin, J. B. Staunton, and S. S. A. Razee (unpublished).
- ⁵E. Bruno and B.L. Gyorffy, *Phys. Rev. Lett.* **71**, 181 (1993).
- ⁶G. Andersson, B. Hjörvarsson, and H. Zabel, *Phys. Rev. B* **55**, 1774 (1997).
- ⁷B. Hjörvarsson, J.A. Dura, P. Isberg, T. Watanabe, T.J. Udovic, G. Andersson, and C.F. Majkrzak, *Phys. Rev. Lett.* **79**, 901 (1997).
- ⁸D. Laberge, C. Sutter, H. Zabel, B. Hjörvarsson, *J. Magn. Magn. Mater.* **192**, 238 (1999); A. Remhof, D. Laberge, G. Song, C. Sutter, K. Theis-Bröhl, H. Zabel, B. Hjörvarsson, *ibid.* **198-199**, 264 (1999).
- ⁹G.R. Harp, S.S.P. Parkin, W.L. O'Brien, and B.P. Tonner, *Phys. Rev. B* **51**, 3293 (1995).
- ¹⁰M.M. Schwickert, R. Coehoorn, M.A. Tomaz, E. Mayo, D. Lederman, W.L. O'Brien, Tao Lin, and G.R. Harp, *Phys. Rev. B* **57**, 13 681 (1998).
- ¹¹R. Coehoorn, *J. Magn. Magn. Mater.* **151**, 341 (1995).
- ¹²J. Izquierdo, A. Vega, O. Elmouhssine, H. Dreyssé, and C. Demangeat, *Phys. Rev. B* **59**, 14 510 (1999).
- ¹³S. Ostanin, V.M. Uzdin, C. Demangeat, J.M. Wills, M. Alouani, and H. Dreyse, *Phys. Rev. B* **61**, 4870 (2000).
- ¹⁴D. Guenzburger, D.E. Ellis, and J.A. Danon, *J. Magn. Magn. Mater.* **59**, 139 (1986).
- ¹⁵A. Broddelfalk, P. Nordblad, P. Blomquist, P. Izberg, R. Wäppling, O. Le Bacq, and O. Eriksson, *J. Magn. Magn. Mater.* **241**, 260 (2002).
- ¹⁶O. Le Bacq, O. Eriksson, B. Johansson, P. James, and A. Delin, *Phys. Rev. B* **65**, 134430 (2002).
- ¹⁷S.U. Jen and G.Y. Chen, *J. Magn. Magn. Mater.* **204**, 165 (1999).
- ¹⁸S.S.A. Razee, J.B. Staunton, and F.J. Pinski, *Phys. Rev. B* **56**, 8082 (1997).
- ¹⁹S.S.A. Razee, J.B. Staunton, B. Ginatempo, F.J. Pinski, and E. Bruno, *Phys. Rev. Lett.* **82**, 5369 (1999).

- ²⁰H.J.F. Jansen, Phys. Rev. B **59**, 4699 (1999).
- ²¹P. James, O. Eriksson, O. Hjortstam, B. Johansson, and L. Nordstrom, Appl. Phys. Lett. **76**, 915 (2000).
- ²²A. R. Mackintosh and O. K. Andersen, in *Electrons at the Fermi Surface*, edited by M. Springfold (Cambridge University Press, Cambridge, 1980); M. Weinert, R.E. Watson, and J.W. Davenport, Phys. Rev. B **32**, 2115 (1985).
- ²³R. C. O'Handley, *Modern Magnetic Materials Principles and Applications* (Wiley, New York, 2000).
- ²⁴O. Hjortstam, K. Baberschke, J.M. Wills, B. Johansson, and O. Eriksson, Phys. Rev. B **55**, 15 026 (1997).
- ²⁵L. Fast, J.M. Wills, B. Johansson, and O. Eriksson, Phys. Rev. B **51**, 17 431 (1995).
- ²⁶A.J. Freeman, R.Q. Wu, M.Y. Kim, and V.I. Gavrilenko, J. Magn. Mater. **203**, 1 (1999).
- ²⁷R. Wu and A.J. Freeman, J. Appl. Phys. **79**, 6209 (1996).
- ²⁸J. Trygg, B. Johansson, O. Eriksson, and J.M. Wills, Phys. Rev. Lett. **75**, 2871 (1995).
- ²⁹I. Yang, S.Y. Savrasov, and G. Kotliar, Phys. Rev. Lett. **87**, 216405 (2001).
- ³⁰E.W. Lee, Rep. Prog. Phys. **18**, 184 (1955).
- ³¹I. Mirebeau, G. Parette, and J.W. Cable, J. Phys. F: Met. Phys. **17**, 191 (1987).
- ³²D.D. Johnson, F.J. Pinski, and J.B. Staunton, J. Appl. Phys. **61**, 3715 (1987).
- ³³M.F. Ling, J.B. Staunton, and D.D. Johnson, J. Phys.: Condens. Matter **7**, 1863 (1995).
- ³⁴D. G. Pettifor, *Bonding and Structure of Molecules and Solids* (Oxford University Press, Oxford, 1995).
- ³⁵F. Ducastelle, *Order and Phase Stability in Alloys* (North-Holland, Amsterdam, 1991).
- ³⁶J.B. Staunton, D.D. Johnson, and B.L. Gyorffy, J. Appl. Phys. **61**, 3693 (1987).
- ³⁷E. du Tremolét de Lacheisserie, *Magnetostriction: Theory and Applications of Magnetoelasticity* (CRC Press, Boca Raton, 1993).